IEEE Robotics and Automation Letters (RAL) paper presented at
2024 IEEE/RSJ International Conference on Intelligent Robots and Systems (IROS)
October 14-18, 2024. Abu Dhabi, UAE

Design of an Accordion-Fold-Inspired Soft Electrohydraulic Actuator for Angular Motion

Sohyun Kim[1], *Student Member*, IEEE, Yenee Oh[2], Joohyeon Kang[3], and Youngsu Cha[1,*], *Senior Member*, IEEE

***Abstract*— Angular motion of soft actuators is important for utilization in robotic systems. In the robots, the angular motion should enable agile movement and a wide range. This study proposes a novel design of a soft electrohydraulic actuator inspired by an accordion with an improved angular deformation range. The actuator generates instantaneous hydraulic force and achieves a fast response within 0.15 s upon activation. Furthermore, the accordion-fold structure of the actuator induces large rotational deformations of 171 degrees. We conduct a series of experiments to investigate the angular motion characteristics from the geometrical parameters of the actuator. Additionally, based on the experimental results, we demonstrate how to apply electrohydraulic actuators to animate objects.**

I. Introduction

Soft robotic systems have inherent advantages in flexibility and versatility of motion by incorporating soft materials into their design [1]. These characteristics enable safe interaction and competent collaboration in industrial work and animated objects [2], [3]. As an essential element in developing soft robots, soft actuators achieve the desired actuation through deformable bodies [4]. They occasionally require complex angular motions such as bending and rotation to cooperate effectively in additional applications. Similarly, soft actuators require agile movements and a wide range of complex angular motions [5], [6].

Several researchers have proposed diverse design methods for generating angular motion and enhancing the performance of soft actuators. Soft actuators with an assembly of multiple chambers have been presented [7], [8], [9]. The rectangular chambers of the actuator are interconnected in a particular shape owing to its natural angular motion [7]. The actuators present various angular motion trajectories as their arrangement patterns change [9]. Origami is another design technique adopted to improve angular performance [10], [11], [12], [13], [14]. The actuator is formed by folding a tube to create cooperative expandable parts [13]. The origami pattern-inspired skeleton is inserted into the actuator to guide programmable actuation [14]. Using multiple components or folding-based assembly techniques is a good strategy for improving actuation properties.

Soft actuators that use smart materials are another candidate for achieving improved performance. For example, various soft actuators with angular capabilities were developed including soft pneumatic actuators (SPAs), dielectric elastomer actuators (DEAs), and shape memory alloys (SMAs). The SPAs are activated by air pressure, and angular motion is induced by drawing a fluid network or attaching an inextensible strain-limiting layer [15], [16], [17], [18], [19], [20], [21], [22], [23], [24], [25]. As air pressure varies, the entire soft body produces angular motion from asymmetric deformation. In the case of DEAs, the response to external electrical drives and the deformation of elastomers are transferred to the total angular motion of the actuators according to their connections to supporting frames [26], [27]. The SMAs embedded in the flexible matrix are deformed and returned to their programmed angular shapes under the thermal source [28]. However, the SPAs require a bulky external air compressor. The DEAs must be pre-stretched, and the SMAs need heating and cooling sources.

Recently, electrohydraulic actuators have been studied as a solution to these challenges [15], [16], [17], [18], [19], [20], [21], [22], [23], [24], [25]. These actuators operate using electrical inputs without an external hydraulic compressor. Based on electrostatic and hydraulic forces, they exhibit immediate actuation and ease of control. The actuators are driven by the voltage signals applied to the electrodes [15]. The actuators deform through the redistribution of the dielectric fluid inside the pouch. By varying the design of the actuator, rotational movements have been reported. Therein,

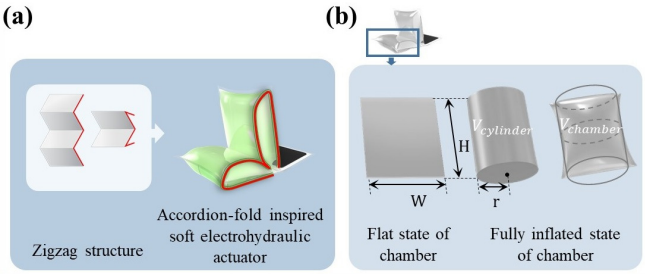

Fig. 1. Concept of accordion-fold inspired soft electrohydraulic actuator. (a) Design schematic of accordion-fold-inspired structure. (b) Concept image for calculating the fully inflated volume of the chamber in the accordion-fold-inspired structure.

This work was supported by the National Research Foundation of Korea (NRF) through the Ministry of Science and ICT (MSIT), Korean Government under Grant 2022M3C1A3098746. (*Corresponding author: Youngsu Cha)

[1]S. Kim and Y. Cha are with School of Electrical Engineering, Korea University, Seoul 02841, Republic of Korea (e-mail: sohyun1224@korea.ac.kr; ys02@korea.ac.kr)

[2]Y. Oh is with School of Mechanical Engineering, Korea University, Seoul 02841, Republic of Korea (e-mail: 12sure@korea.ac.kr)

[3]J. Kang is with Department of Smart Convergence, Korea University, Seoul 02841, Republic of Korea (e-mail: kangzoo99@korea.ac.kr)

the electrohydraulic actuators with asymmetric electrodes produce the rotational trajectory with an active plate by generating two tilts [21]. However, the angle of the slope is limited to an acute angle. Unidirectional and bidirectional bending motions have been developed by attaining strain-limited substrates [22], [24]. The ranges of motions are also restricted as part of the input energy is converted into strain energy of the substrates [25]. To generate large angular movements without an additional substrate, a novel design approach is required for soft electrohydraulic actuators.

In this paper, we propose a soft electrohydraulic actuator design for a wider range of angular motions. Inspired by accordions, the actuator can be easily fabricated from a single sheet without any stiffening layers or additional parts. The accordion-fold design results in fast and large angular deformation of the electrohydraulic actuator. Furthermore, the angular motion of the actuator is characterized and evaluated using various geometric parameters, dielectric fluid volume, and input voltage. Finally, the proposed actuator is demonstrated as animated objects.

II. Methods

A. Design

The novel design of the soft electrohydraulic actuator is based on a unique pouch inspired by the accordion-fold (Fig. 1(a)). The accordion-fold has a zigzag structure with units repeated at equal intervals, similar to the accordion bellows. The zigzag structure enables the number of chambers in the pouch to be expanded and is used as a tool to change the operational behavior of the pouch actuator [7]. We adopt the zigzag structure exhibiting the accordion-fold method to design the pouch. The proposed pouch design using an accordion-fold can provide exceptional angular motion and an improved range of motion when inflated.

In an accordion-fold pouch, the zigzag structure acts as an inflatable fluid chamber (Fig. 1(b)). Here, we derive the volume of liquid required to fill the pouch from the geometry of each fully inflated chamber. Each chamber initially has a flat rectangular shape with W in width and H in height. The fully inflated chamber is assumed to be cylindrical after the operation, and the volume of the cylinder ($V_{cylinder}$) is calculated using $\pi r = W$ [15] as

$$V_{cylinder} = \pi \times r^2 \times H = \pi \times (\frac{W}{\pi})^2 \times H = \frac{W^2}{\pi} H \quad (1)$$

where r is the radius of the cross-section when fully inflated. However, experimental observations show that the actual inflation volume for a rectangular chamber is lower than the ideal prediction, and this is called the "paper bag" problem [29], [30]. With consideration of the issue, the relationship between the volume of the chamber ($V_{chamber}$) and the cylinder is expressed as

$$V_{chamber} = V_{cylinder} - V_{loss} \quad (2)$$

where V_{loss} is the volume difference between $V_{chamber}$ and $V_{cylinder}$. The value has been reported from experimental finding as [29], [30]

$$V_{loss} = 0.142W^3(1 - 10^{-\frac{H}{W}}). \quad (3)$$

Applying this equation, the maximum inflation volume of the chamber is rewritten as

$$V_{chamber} = \frac{W^2}{\pi} H - 0.142W^3(1 - 10^{-\frac{H}{W}}). \quad (4)$$

Therefore, the fluid volume required to fill an accordion-fold pouch is obtained as the sum of the fully inflated volumes of the two chambers.

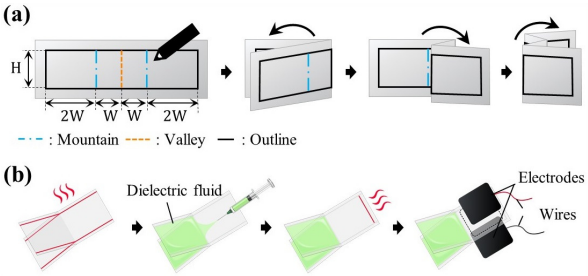

Fig. 2. Fabrication process of accordion-fold-inspired soft electrohydraulic actuator. (a) Manufacturing accordion-fold-inspired pouch using a sheet of film. (b) Process of heat sealing the film for injecting dielectric fluid and attaching electrodes and wires.

B. Fabrication

The simple fabrication process of the soft electrohydraulic actuator focuses on achieving accordion-fold-inspired structures (Fig. 2(a)). A single sheet of biaxially oriented polypropylene (BOPP) film (25 μm, Biztem Co., Ltd.) was used for this design. Patterns of two mountain lines, one valley line, and an outline were drawn on the film. The length of each line is expressed as W and H, and the dimensions of the rectangular chamber are characterized as $W \times H$. The BOPP film was folded alternately in accordion-folds with the designed patterns.

The actuator was fabricated by sealing the folded film using a heat bonding machine (Impulse Hand Sealer SK-210, SAM-BO TECH Co., Ltd.) (Fig. 2(b)). The overlapping film was sealed to a width of 2 mm along the outline except at the fluid inlet to form a pouch. FR3 oil (FR3 natural ester dielectric fluid, Cargill) was used as the dielectric fluid and was injected into the pouch through an inlet. The volume of the injected fluid was determined by summing the volume into which the two chambers of the accordion-fold-inspired structure could fully expand, based on equation (4). After the air bubbles were removed from the inside of the pouch, the injection port was heat bonded using the same method to seal the pouch completely. The surfaces of half of the pouch were covered with conductive carbon tapes (Nis-shin EM.CO., Ltd.) as flexible electrodes. The electrodes were cut into rectangular shapes utilizing a cutting machine (Silhouette Cameo, Silhouette America Co., Inc.). Their dimensions were designed with margins of 0.2 and 0.4 cm for the width and height of the area, respectively. Each vertex of the electrodes was rounded off to prevent electrical

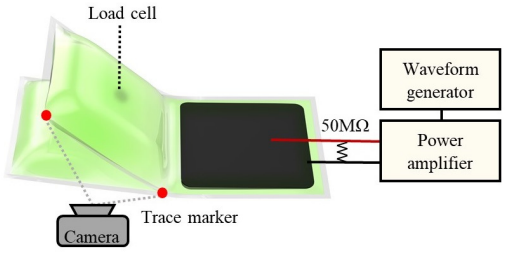

Fig. 3. Experimental setup and circuit configuration of accordion-fold-inspired soft electrohydraulic actuator.

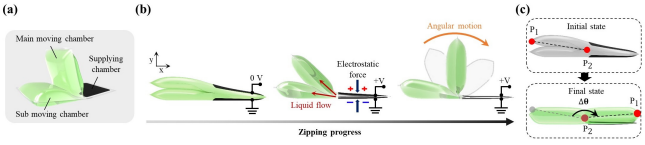

Fig. 4. Mechanism of accordion-fold-inspired soft electrohydraulic actuator. (a) Designation of components. (b) Operation mechanism according to zipping progress. (c) Position definition for angular motion measurement.

shortening. Finally, a pair of stripped wires were connected to the electrodes to apply a voltage to the actuator.

C. Experimental Setup

The experimental setup of the accordion-fold-inspired soft electrohydraulic actuator is shown in Fig. 3. A power amplifier (MK-200002B, MKPOWER., Inc.) with an input voltage of 10 kV is applied to the electrodes of the actuator. The input signal was governed by a waveform generator (33500B series, Keysight Technologies Co., Inc.). A total of 50 MΩ resisters were connected between the ports of the power amplifier to discharge the electrodes. An optical camera (DSC-RX100M7, Sony Co., Inc.) was used to observe the angular motion of the actuator from a front view. Images were recorded at 60 or 960 fps. The trace markers (Jong Ie Nara.) made of paper were attached to the tips of the actuators. The acquired data were processed through a motion analysis software (ProAnalyst Motion Analysis Software, Xcitex, Inc.). In addition, to measure the blocking force of the actuator, we utilized a load cell (GS0-500, Transducer Techniques.). The measurement point was located at the center of the accordion-fold-inspired structure. The quantified voltage from the load cell was amplified using an amplifier unit (IL-1000 amplifier unit, Keyence Co.). A data acquisition board (NI 9229, National Instruments Co.) received the voltage signal and transferred it to a PC at 2000 Hz.

D. Operation Mechanism

The accordion-fold-inspired soft electrohydraulic actuator comprised two moving chambers and a supplying chamber (Fig. 4(a)). The two moving chambers are connected through a common axis and divided into main moving chamber and sub moving chamber. The proposed electrohydraulic

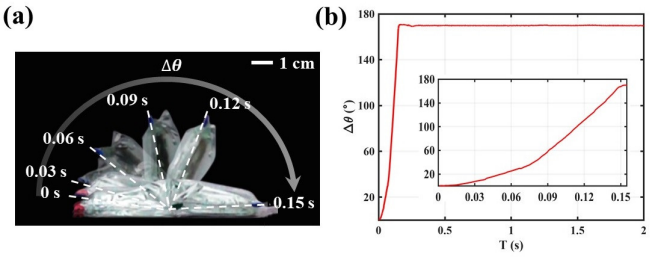

Fig. 5. Angular motion of accordion-fold-inspired soft electrohydraulic actuator. (a) Time-lapse photograph of moving chambers. (b) Time trajectory of the rotation angle of the main moving chamber. Specific time trajectory rotation angle for operating time of 0.15 s is inserted as inset plot.

actuators convert the inflation motion of these chambers into the angular motion of the main moving chamber to produce a large angular motion.

The basic concept of the proposed soft electrohydraulic actuator is the generation of pouch movements using electrostatic and hydraulic forces when a voltage is applied [15], [16]. The actuator was initially at rest with zero input voltage (Fig. 4(b)). As the input voltage was applied to the electrodes of the supplying chamber, the Maxwell stress began to progressively zip the electrodes from the edge [31]. The dielectric fluid is pushed from the supplying chamber to the moving chambers by an electrostatic force. Subsequently, the cross-section swelled owing to the increased pressure in the main and sub moving chambers. Changes in the shape of the inflated chambers pushed each other and motivated angular motion. The accordion-fold method produced an angular motion of the main moving chamber as the moving chambers expanded and unfolded.

The angle was measured based on the trace markers attached to the endpoints P_1 and P_2 of the main moving chambers of the actuator (Fig. 4(c)). The rotation angle ($\Delta\theta$) was defined as the angle by which the $\overline{P_1P_2}$ was rotated between the initial and final states. The maximum range of possible angular motion owing to the unique structure of the actuator was within approximately 180°.

III. RESULTS

A. Angular Motion of Actuator

The angular motion of an accordion-fold-inspired soft electrohydraulic actuator was tested. The actuator was fabricated with a width and height of 4 cm for both the moving and supplying chambers. An input voltage with an amplitude of 10 kV was used in the experiment. The movements of the actuator were captured at a rate of 960 fps for detailed observation in slow-motion mode, and six pictures were overlapped at 0.03 s intervals (Fig. 5(a)). When the input voltage was applied to the actuator, the main and sub moving chambers swelled and pushed each other. The main moving chamber produced a gradual clockwise angular motion along the accordion-folded valley crease. The main moving chamber took approximately 0.15 s to flip within the maximum rotation range of the actuator completely.

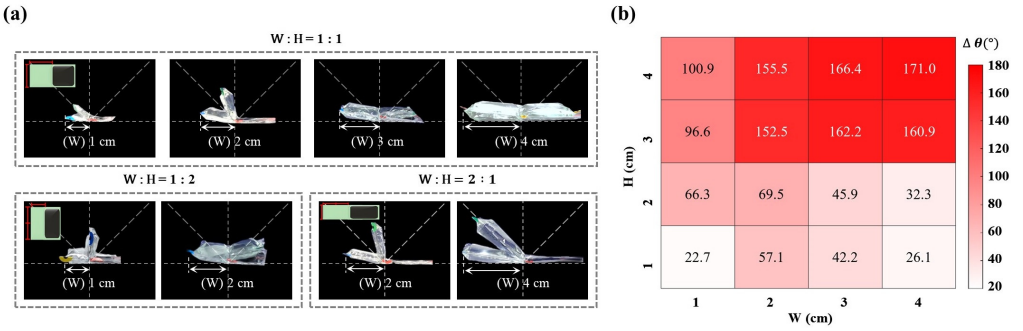

Fig. 6. Angular motion of accordion-fold-inspired soft electrohydraulic actuator with variance of width and height of all chambers. (a) Snapshots at peak angular movement for three different aspect ratios. Gray dashed lines represent the angles of 0, 45, 90, 135, 180°. (b) Heat map of the angles of 16 actuators with variance of the width and height.

In addition, we plotted the time responses of the angle variation over 2 s recorded from the operation of the actuator as the input voltage (Fig. 5(b)). The rotation angle of the main moving chamber increased rapidly until it reached a maximum angle of 171°, and this angle was maintained. The accordion-fold design demonstrated the ability to convert inflation deformation into the angular motion of the main moving chamber and achieved an improved rotation range.

B. Effect of Geometrical Parameters

The geometrical parameters of the accordion-fold-inspired soft electrohydraulic actuator can be used as key tools to improve the angular performance. We performed angular motion by varying the design parameters width (W) and height (H) of each chamber to investigate the effects of the geometric configuration. Actuators were fabricated with increasing widths as multiples for three different aspect ratios as W:H = 1:1, 1:2, and 2:1. The same voltage was applied, and the appearance of the peak angular movement was captured (Fig. 6(a)). At the same ratios of 1:1 and 1:2, the angles of the main moving chambers gradually increased as the width increased. For a 2:1 aspect ratio, the angles of the main moving chambers decreased as the width increased. When the width was less than or equal to the height ($W \leq H$), increasing the size of the chambers while maintaining the same aspect ratio was accompanied by an improvement in the rotation angle. Conversely, when the width was greater than the height ($W > H$), the correlation between the size and the output angle was not constant. These trends were probably because of the progressive zipping mechanism of the electrodes [32], [33]. Therefore, it was desirable, such that the height of the chamber was designed to be at least larger than or equal to the width [34], [35].

Moreover, we tested the angular motion of the main moving chambers of the proposed actuators of various sizes to investigate their optimal performance. A total of 16 actuators were fabricated by varying the width and height of the chamber from 1 to 4 cm in 1 cm increments. When the same input voltage was applied, the measured angles of the main moving chambers were represented in a heat map (Fig. 6(b)). By comparing actuators with equal areas of

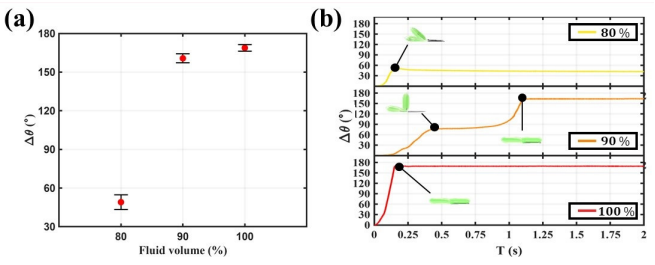

Fig. 7. Angular motion of accordion-fold-inspired soft electrohydraulic actuator with a variation of internal dielectric fluid volume. (a) Rotation angles of main moving chambers. Red points are averages of ten trials, and black error bars represent standard deviations. (b) Time trajectories of rotation angles of main moving chambers.

electrodes, all designs with shorter widths than their height exhibited higher angular motion than those that did not. For example, the angle at 1×2 cm was 13.9% higher than at 2×1 cm, and the value at 2×4 cm was 79.2% higher than that at 4×2 cm. These designs with a height longer than the width were advantageous enhanced rotation angles, as suggested above. In addition, the 10 actuators that satisfied the proposed design conditions ($W \leq H$) exhibited improved angular motion as the size increased. At the same height, the rotation angle increased with increasing width. Similarly, the angle increased with increasing height for the same width. Consequently, the angular movement of the main moving chamber produced a minimum of 22.7° and a maximum of 171°. The maximum motion was decided to have been reached if the main moving chambers were greater than 150°. These results demonstrate that the moving chamber of the actuator achieves superior angular performance.

C. Effect of Fluid Volume

The performance of accordion-fold-inspired soft electrohydraulic actuator can also be affected by the volume of the injected fluid, as they are actuated in a limited volume with an internal dielectric fluid. To optimize the motion performance of the actuator, the rotation angles of the main moving chambers were investigated by varying the amount of fluid used (Fig. 7(a)). The size parameters of the actuator, width,

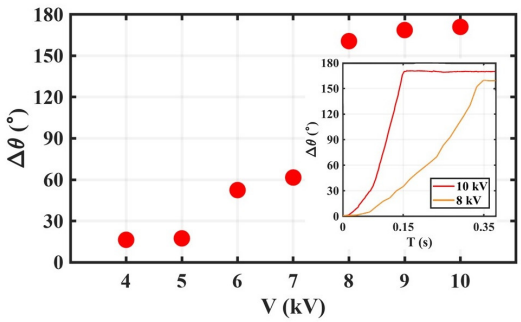

Fig. 8. Angular motion of accordion-fold-inspired soft electrohydraulic actuator with variance of input voltage. Red points are rotation angles of the main moving chamber. Comparison with time trajectories of rotation angles at 8 and 10 kV are inserted as inset plot.

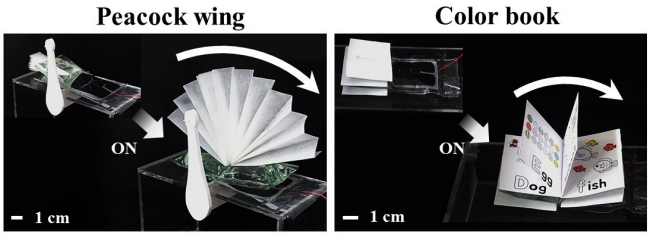

Fig. 9. Animated objects using an accordion-fold-inspired soft electrohydraulic actuator. Peacock wing was spread, and color book was opened when input voltages were applied.

and height, were set to 4 cm to generate the largest rotation angle from Section II-B. The fluid volumes of the actuator were determined to be 80, 90, and 100% of the sum of the fully inflated moving chambers. Under identical experimental conditions, angular motion tests were conducted in sets of 10 repetitions for each fabricated actuator. The mean and standard deviation of the angles were calculated. The average rotation angles were 49.0, 160.7, and 168.8° at each rate. The angles at 90 and 100% increased significantly compared to those at 80%, reaching an almost flat state. Fluid volumes less than the full inflation of the moving chambers produced a smaller angle because each moving chamber did not expand uniformly, even if the supplying chamber was zipped entirely. Therefore, we found that the actuator achieved the most effective angular motion when the two moving chambers were fully inflated with the fluid inside.

To compare the motion response according to the injected fluid volume in detail, the angular motions of the proposed actuators were analyzed concerning the time trajectories (Fig. 7(b)). Data were collected at 960 fps for 2 s after an input voltage was applied. In the case of 80%, the main moving chamber rotated approximately 50° in 0.2 s. Meanwhile, the rotated angle of the main moving chamber with a 90% rate increased monotonically into two sections over a longer period. In the first section, the chamber rotated approximately 80° in 0.4 s and maintained its upright shape for approximately 0.3 s. When the second section is reached, the main moving chamber results in a final movement of approximately 160° with further rotation. It took approximately 1.1 s to complete a reachable rotation. In contrast, the main moving chamber with a 100% rate produced an angular motion over 170° within a rapid actuation time of approximately 0.15 s. From the operating time perspective, a rate of 100% demonstrated a faster response even though both 90 and 100% achieved the maximum rotational range. These results indicate that the angular motion was more effective in the case with an injected fluid equal to the fully inflated volume of both moving chambers than in the other case.

D. Effect of Input Voltage

The accordion-fold-inspired soft electrohydraulic actuator generated a controllable angular motion depending on the input voltage applied to the electrodes. The rotation angles of the main moving chamber were investigated to evaluate their performance concerning the applied voltage (Fig. 8). The actuator had design parameters of width and height as 4 cm and was manufactured with an injected fluid rate of 100%. The input voltage was increased in 1 kV increments from 4 to 10 kV to produce meaningful angles. Voltages below 4 kV did not reach the critical point for the zipping process via electrostatic forces. The rotational angles at 4, 6, 8, and 10 kV were 16.4, 52.5, 160.6, and 171.0°, respectively. As the input voltage increased, the actuator produced an improved angular motion by progressive zipping until the maximum inflation of moving chambers was reached. Voltages higher than 8 kV were achieved in the range of maximum angular motion. Within the range, 8 and 10 kV inputs took approximately 0.35 and 0.15 s to complete rotation, respectively. The results indicate that a relatively high voltage is advantageous for a faster actuation time of an actuator with larger angular motion.

E. Animated Object Application

The proposed soft electrohydraulic actuator achieved advanced angular motion using an accordion-fold-inspired design. This operation of the actuator can be applied to animate objects in various fields (Fig. 9). Based on the optimized design from the experimental results, an actuator with a width and height of 4 cm and fluid rate of 100% was adopted for the demonstration. An actuator is used to represent the motion of the peacock wing spread. The wing was initially folded between two moving chambers. When voltage was applied, the model wing spread as the main moving chamber underwent angular deformation. Similarly, we demonstrate the opening of a color book. All pages of the book were opened together by the input signal, and then the pictures on each page were exhibited. The rapid and wide angular movements of the main moving chamber induced striking animations in both cases. The supplementary video shows these demonstrations. We comment that the unique design of the actuator enables extended angular motions in animated objects.

IV. CONCLUSIONS

In this study, we presented a novel design for a soft electrohydraulic actuator that performed a wider range of angular motions. The proposed actuator offered a compact chamber design, a simple manufacturing process, and significant angular motion by the accordion-inspired method. The size of the chambers could be easily scaled up or down through a simple manufacturing process. The design method presented in this study investigated the effects of aspect ratio, inflation volume, and input voltage on the generated rotation angle. The actuator produced a maximum angular displacement of 171°(almost flat) in a rapid time of 0.15 s when the width and height of the chamber were the same and sufficiently large. Fast and large angular movements of electrohydraulic actuators were demonstrated through animated objects. This simple and effective design technique provides important insights into soft robotics.

REFERENCES

[1] D. Rus and M. Tolley, "Design, fabrication and control of soft robots," *Nature*, vol. 521, pp. 467–475, 2015.

[2] R. Niiyama, X. Sun, L. Yao, H. Ishii, D. Rus, and S. Kim, "Sticky actuator: free-form planar actuators for animated objects," in *Proceedings of the ninth international conference on tangible, embedded, and embodied interaction*, 2015, pp. 77–84.

[3] K. Narumi, H. Sato, K. Nakahara, Y. Seong, K. Morinaga, Y. Kakehi, R. Niiyama, and Y. Kawahara, "Liquid pouch motors: printable planar actuators driven by liquid-to-gas phase change for shape-changing interfaces," *IEEE Robotics and Automation Letters*, vol. 5, pp. 3915–3922, 2020.

[4] N. El-Atab, R. Mishra, F. Al-Modaf, L. Joharji, A. Alsharif, H. Alamoudi, M. Diaz, N. Qaiser, and M. M. Hussain, "Soft actuators for soft robotic applications: a review," *Advanced Intelligent Systems*, vol. 2, p. 2000128, 2020.

[5] S. Li, J. Lin, H. Kang, Y. Cheng, and Y. Chen, "Bio-inspired origamic pouch motors with a high contraction ratio and enhanced force output," *Robotics and Autonomous Systems*, vol. 149, p. 103983, 2022.

[6] Y. Wang, Z. Ma, S. Zuo, and J. Liu, "A novel wearable pouch-type pneumatic artificial muscle with contraction and force sensing," *Sensors and Actuators A: Physical*, vol. 359, p. 114506, 2023.

[7] J. Fang, J. Yuan, M. Wang, L. Xiao, J. Yang, Z. Lin, P. Xu, and L. Hou, "Novel accordion-inspired foldable pneumatic actuators for knee assistive devices," *Soft Robotics*, vol. 7, pp. 95–108, 2020.

[8] R. Natividad, M. Del Rosario, P. C. Y. Chen, and C. Yeow, "A reconfigurable pneumatic bending actuator with replaceable inflation modules," *Soft Robotics*, vol. 5, pp. 304–317, 2018.

[9] H. Lee, N. Oh, and H. Rodrigue, "Expanding pouch motor patterns for programmable soft bending actuation: enabling soft robotic system adaptations," *IEEE Robotics and Automation Magazine*, vol. 27, pp. 65–74, 2020.

[10] L. Paez, G. Agarwal, and J. Paik, "Design and analysis of a soft pneumatic actuator with origami shell reinforcement," *Soft Robotics*, vol. 3, pp. 109–119, 2016.

[11] C. Thalman, Q. Lam, P. Nguyen, S. Sridar, and P. Polygerinos, "A novel soft elbow exosuit to supplement bicep lifting capacity," in *2018 IEEE/RSJ International Conference on Intelligent Robots and Systems (IROS)*, 2018, pp. 6965–6971.

[12] H. Yap, P. Khin, T. Koh, Y. Sun, X. Liang, J. Lim, and C. Yeow, "A fully fabric-based bidirectional soft robotic glove for assistance and rehabilitation of hand impaired patients," *IEEE Robotics and Automation Letters*, vol. 2, pp. 1383–1390, 2017.

[13] W. Felt, "Folded-tube soft pneumatic actuators for bending," *Soft Robotics*, vol. 6, pp. 174–183, 2019.

[14] S. Li, D. M. Vogt, D. Rus, and R. J. Wood, "Fluid-driven origami-inspired artificial muscles," *Proceedings of the National Academy of Sciences*, vol. 114, pp. 13 132–13 137, 2017.

[15] N. Kellaris, V. Venkata, G. Smith, S. Mitchell, and C. Keplinger, "Peano-HASEL actuators: muscle-mimetic, electrohydraulic transducers that linearly contract on activation," *Science Robotics*, vol. 3, p. 3276, 2018.

[16] P. Rothemund, N. Kellaris, S. Mitchell, E. Acome, and C. Keplinger, "HASEL artificial muscles for a new generation of lifelike robots—recent progress and future opportunities," *Advanced materials*, vol. 33, p. 2003375, 2021.

[17] S. Mitchell, X. Wang, E. Acome, T. Martin, K. Ly, N. Kellaris, V. Venkata, and C. Keplinger, "An easy-to-implement toolkit to create versatile and high-performance HASEL actuators for untethered soft robots," *Advanced Science*, vol. 6, p. 1900178, 2019.

[18] N. Kellaris, P. Rothemund, Y. Zeng, S. Mitchell, G. Smith, K. Jayaram, and C. Keplinger, "Spider-inspired electrohydraulic actuators for fast, soft-actuated joints," *Advanced Science*, vol. 8, p. 2100916, 2021.

[19] Purnendu, S. Novack, E. Acome, C. Keplinger, M. Alistar, M. Gross, C. Bruns, and D. Leithinger, "Electriflow: soft electrohydraulic building blocks for prototyping shape-changing interfaces," in *Proceedings of the 2021 ACM Designing Interactive Systems Conference*, 2021, pp. 1280–1290.

[20] A. Washington, J. Su, and K. Kim, "Actuation behavior of hydraulically amplified self-healing electrostatic (HASEL) actuator via dimensional analysis," *Actuators*, vol. 12, p. 208, 2023.

[21] S. Kim and Y. Cha, "Rotary motion and manipulation using electrohydraulic actuator with asymmetric electrodes," *IEEE Robotics and Automation Letters*, vol. 5, pp. 3945–3951, 2020.

[22] S. Kim and Y. Cha, "Electrohydraulic actuator based on multiple pouch modules for bending and twisting," *Sensors and Actuators A: Physical*, vol. 337, p. 113450, 2022.

[23] S. Kim and Y. Cha, "A soft crawling robot with a modular design based on electrohydraulic actuator," *iScience*, vol. 26, p. 106726, 2023.

[24] T. Park, K. Kim, S. Oh, and Y. Cha, "Electrohydraulic actuator for a soft gripper," *Soft Robotics*, vol. 7, pp. 68–75, 2020.

[25] K. Lee and Y. Cha, "Quasi-static analysis of an electrohydraulic actuator for a soft gripper," *Sensors and Actuators A: Physical*, vol. 352, p. 114214, 2023.

[26] J. Li, L. Liu, Y. Liu, and J. Leng, "Dielectric elastomer spring-roll bending actuators: applications in soft robotics and design," *Soft Robotics*, vol. 6, pp. 69–81, 2019.

[27] G. Lau, K. Heng, A. Ahmed, and M. Shrestha, "Dielectric elastomer fingers for versatile grasping and nimble pinching," *Applied Physics Letters*, vol. 110, p. 182906, 2017.

[28] W. Wang, H. Rodrigue, H. Kim, M. Han, and S. Ahn, "Soft composite hinge actuator and application to compliant robotic gripper," *Composites Part B: Engineering*, vol. 98, pp. 397–405, 2016.

[29] A. Robin, "Paper bag problem," *Mathematics Today-Bulletin of the Institute of Mathematics and its Applications*, vol. 40, pp. 104–107, 2004.

[30] B. Do, A. Okamura, K. Yamane, and L. Blumenschein, "Macro-mini actuation of pneumatic pouches for soft wearable haptic displays," in *2021 IEEE International Conference on Robotics and Automation (ICRA)*, 2021, pp. 14 499–14 505.

[31] L. Maffli, S. Rosset, and H. Shea, "Zipping dielectric elastomer actuators: Characterization, design and modeling," *Smart Materials and Structures*, vol. 22, p. 104013, 2013.

[32] R. Diteesawat, T. Helps, M. Taghavi, and J. Rossiter, "Electro-pneumatic pumps for soft robotics," *Science Robotics*, vol. 6, p. 3721, 2021.

[33] P. Rothemund, N. Kellaris, and C. Keplinger, "How inhomogeneous zipping increases the force output of Peano-HASEL actuators," *Extreme Mechanics Letters*, vol. 31, p. 100542, 2019.

[34] A. Veale, S. Xie, and I. Anderson, "Characterizing the Peano fluidic muscle and the effects of its geometry properties on its behavior," *Smart Materials and Structures*, vol. 25, p. 065013, 2016.

[35] D. Sangian, S. Naficy, G. Spinks, and B. Tondu, "The effect of geometry and material properties on the performance of a small hydraulic McKibben muscle system," *Sensors and Actuators A: Physical*, vol. 234, pp. 150–157, 2015.